Effect of pressure on the atom positions in Se and Te

R. Keller,* W. B. Holzapfel, and Heinz Schulz
Max-Planck-Institut für Festkörperforschung, 7 Stuttgart 80, Federal Republic of Germany
(Received 12 April 1977)

The effect of pressure on atomic positions and lattice parameters is determined for trigonal Se under pressures from 0 to 86 kbar and for trigonal Te from 0 to 40 kbar by single-crystal x-ray diffraction using a diamond anvil high-pressure cell in a standard precession camera. The structural data confirm the lattice-dynamical homology that had been observed in the variation of the Raman frequencies at low pressures. However, the strongly nonlinear variations in the interatomic distances and the bond angles show deviations from a structural homology as the high-pressure phase transitions are approached.

I. INTRODUCTION

α-Se and α-Te, the stable forms at atmospheric pressures, have a trigonal structure with the space group[1,2] $P3_121$-D_3^4 or $P3_221$-D_3^6. Prominent features of these structures are infinite helices parallel to the c axis with three atoms per turn (Fig. 1) at the positions $(u, 0, 0)$. The atomic-position parameter u is related by $u = q/a$ to the radius q of the helices.

The lattice dynamics of these strongly anisotropic structures have been described by several model calculations using either the valence-force-field[3-6] (VFF) or empirical-pseudopotential methods[7] (EPM). These models[3,4] were compared with experimental data, including variations of the lattice parameters a and c,[8] of the Raman frequencies,[9] and of the elastic constants[10] under pressure. Since, however, no data were available on the variation of the third structural parameter, the atomic-position parameter u, all previous discussions had to make one or another assumption about the variation of this parameter under pressure. From a microscopic point of view and by comparison between Se and Te, it appeared to be most reasonable to assume a strong variation in the (next-nearest-neighbor) interchain distance R, a small variation in the (nearest-neighbor) interchain distance r, and no variation in the intrachain angle θ.[9] These assumptions were supported by the close homology that was found for the lattice dynamics of Se and Te.[9,10]

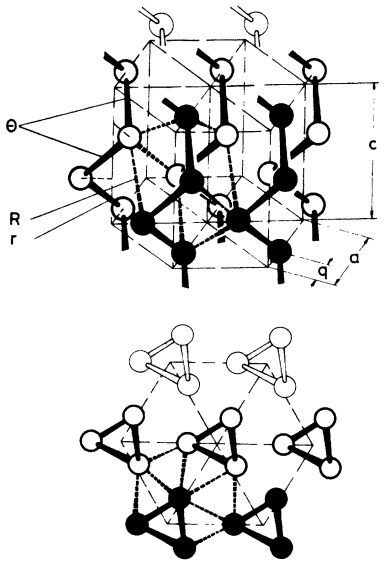

FIG. 1. Structure of trigonal Se and Te.

Integrated intensity measurements of the (100) and (101) x-ray diffraction peaks of polycrystalline Se samples under quasihydrostatic pressures up to 52 kbar indicated, however,[11] that the intrachain angle θ may vary even more than the intrachain distance r under pressure. The accuracy of these measurements was limited by pressure gradients, texture, and the fact that only one intensity ratio had been studied. More accurate results could be expected to be obtained from x-ray diffraction on single crystals under hydrostatic pressures. Details of this technique and experimental results for Se and Te are presented in the next sections. Various aspects of the structural homology in Se and Te and their implications for the lattice-dynamical models are discussed in the last section.

II. EXPERIMENTAL

A. Samples

Crystals of Te had been grown by the Czochralski method and were characterized by a hole concentration of 10^{14} cm^{-3} and a dislocation concentration of 10^4 cm^{-2}.[12] The crystals were cut by an acid saw to plates of about 1 mm thickness parallel to the (201) plane. Diffraction patterns of the $(h0l)$ plane were taken with these crystals. Doukhan acid[13] was used to reduce the thickness of the plate to 0.045 mm, which is optimized for measure-

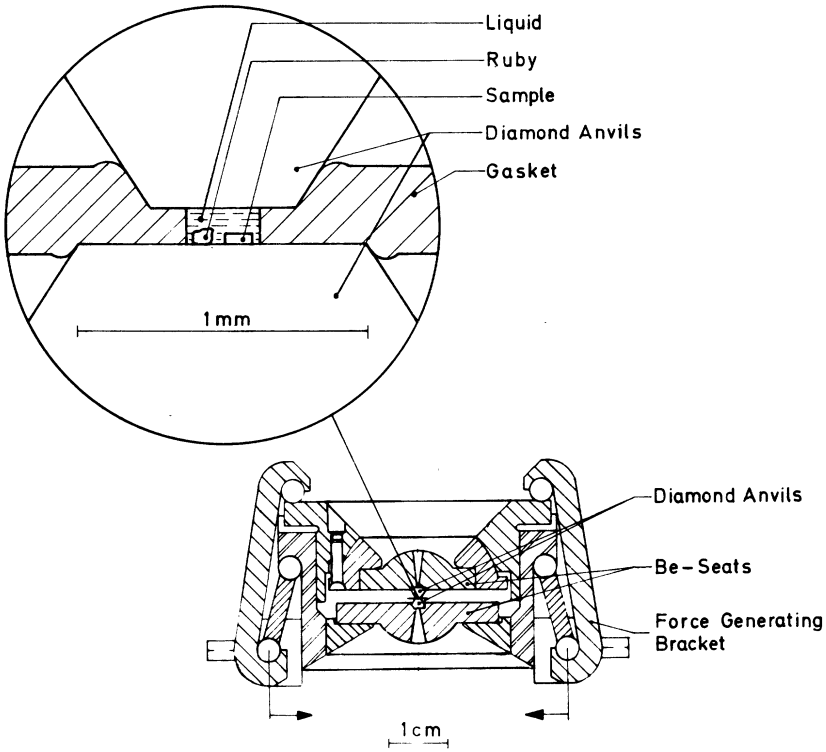

FIG. 2. Diamond anvil cell for x-ray diffraction on single crystals under pressures up to 100 kbar.

ments with Mo $K\alpha$ radiation in the transmission mode. The area of the flakes was further reduced to an appropriate size of $0.11\times0.09\times0.045$ mm^3 to fit into the sample area of the diamond anvil cell (Fig. 2) by cutting with a scalpel. This procedure led to no significant broadening of reflections. The quality of the Te crystals was checked by measurements of the lattice constants at zero pressure. The values $a = 4.456$ Å and $c = 5.923$ Å agreed within the range of the apparative error with the literature values of $a = 4.456$ Å and $c = 5.927$ Å.[1,14]

Crystals of Se had been grown from the gas phase, starting from polycrystalline material, which had been purified by vacuum distillation.[15] One crystal flake was chosen with an appropriate thickness of 0.03 mm. X-ray measurements showed that the plane of the flake was the (110). Pictures of the (*hhl*) reciprocal-lattice plane were obtained with these crystals. The flake was carefully etched down with diluted Na_2S to a size of $0.06\times0.07\times0.03$ mm^3. The etching procedure was carried out by partly covering the flake with silicone oil and etching the free parts away. The chemical reaction could be immediately stopped by a drop of water. We used this more complicated procedure for the Se crystals, since cutting disturbed these crystals so much that no single-crystal x-ray reflections could be detected. The quality of the Se crystals was tested by measurements of the lattice constants at zero pressure, giving the values $a = 4.368$ Å and $c = 4.958$ Å, which are in good agreement with the literature data $a = 4.366$ Å and $c = 4.958$ Å.[1,16]

B. High-pressure technique

The present high-pressure technique is based on recent developments of the diamond anvil high-pressure cell.[17-20] The diamond anvil device used in this study, together with its handling on a precession camera, has been described in detail previously.[21] Figure 2 shows an enlarged view of the steel gasket between the two diamond anvils and the central hole in the steel gasket, which includes the pressure transmission liquid, as well as the single-crystalline sample and a ruby splinter for the pressure determination.[20-24] The accuracy of the pressure determination was ±0.7 kbar with respect to the ruby scale and therefore better than ±0.9 kbar with respect to Decker's equation of state of NaCl.

X-ray intensity measurements on Se were carried out up to 87 kbar. When the pressure was increased above 90 kbar, the crystal was heavily damaged by effects of strain. Most probably, this was caused by solidification of the silicone oil which was used to fix the crystal to one of the dia-

monds.[25] At 100 kbar, only two independent reflections could be identified. These reflections were used for the determinations of the lattice constants at this pressure. In the Te experiment,[26] the first-order phase transition at about 40 kbar limited the pressure range. Three measurements were taken with Te on decreasing pressure. The good agreement between the compression and decompression measurements showed that hysteresis effects could be ignored.

C. X-ray diffraction

For the x-ray diffraction measurements with filtered Mo $K\alpha$ radiation, the diamond anvil device was mounted on a commerical goniometer head in a Stoe precession camera which was used with a crystal to film distance of 75 mm. Experimental details including information about orientation and centering procedures have been given elsewhere.[21,27] A collimator with 0.5 mm diameter was used in front of the high-pressure device. Furthermore, the gasket screened parts of the radiation, which was scattered from the incoming beam in the Be backing. The transmittance of the diamond anvil device for Mo $K\alpha$ was about 15%. The used precession angles were limited by geometry, depending on how much the arcs of the goniometer head had to be moved away from their 0° positions to orient the crystal together with the diamond cell.

The Se experiment was carried out with precession angles of typically 23°. Even with this large angle, only eight independent reflections could be measured in the (hhl) plane.

In the case of Te, up to 25 independent reflections were observed at precession angles up to 20° in the $(h0l)$ plane. However, owing to changes of the crystal orientation under pressure, the precession angles had to be reduced down to 15°. Therefore, only 13 independent reflections could be followed through all the pressure runs on Te.

The x-ray reflection patterns were collected on x-ray film (Agfa Curix RP2). Exposure times of typically 17 h provided a signal-to-noise ratio which was sufficient to identify also the weakest reflections in the (hhl) plane of Se and the $(h0l)$ plane of Te. The diffraction patterns were evaluated with an automatic densitometer (Syntex AD1), which measured the optical density of the x-ray reflection spots on the film. The optical density is proportional to the x-ray intensity as long as the x-ray film is not saturated. Therefore, the optical densities in the center of the strongest x-ray reflections [(003) in Se and (101) in Te] were measured first to guarantee that no saturation occurred.

III. VARIATIONS OF THE LATTICE PARAMETERS

The lattice constants a and c were calculated from the d_{hkl} values by least-squares refinements.[28] Thereby, the complete data sets were used, i.e., eight pairs of reflections for Se and 13–25 for Te. The results are listed in Table I together with calculated a/c and V values. Third-order polynomials,

$$\Delta x/x_0 = A_{x1}p + A_{x2}p^2 + A_{x3}p^3 ,$$

were used for the fit of the high-pressure data. x represents either a, c, or the volume V, Δx is defined by $\Delta x = x - x_0$, x_0 is the value of x at 1 bar, p is the pressure, and the A_{xi} are the adjustable parameters. The A_{xi}'s for Se and Te are tabulated in Table II together with the values for the isothermal compression moduli,

$$B_x = -x_0 \left.\frac{dp}{dx}\right|_{p=0} ,$$

and their pressure dependences,

$$B_x' = \left.\frac{dB_x}{dp}\right|_{p=0} ,$$

at 1 bar. The B_x and B_x' are calculated from the relations

$$B_x = -(A_{x1})^{-1}, \quad B_x' = |2A_{x2}/A_{x1}^2| - 1 .$$

The standard deviations of the least-squares fits are given in parentheses in Table II. The errors

TABLE I. Lattice parameters of trigonal Se and Te under pressure. The numbers in parentheses represent only the standard deviations of the refinements.

	p (kbar)	a (Å)	c (Å)	c/a	V (Å^3)
Se	0	4.368(3)	4.958(4)	1.135	81.92
	1.2	4.343(1)	4.964(2)	1.143	81.09
	25.8	4.052(1)	5.038(3)	1.243	71.64
	41.5	3.956(1)	5.069(2)	1.281	68.70
	49.9	3.910(1)	5.080(1)	1.299	67.25
	65.7	3.846(1)	5.095(2)	1.339	65.25
	77.0	3.810(1)	5.110(2)	1.341	64.22
	86.4	3.779(1)	5.109(2)	1.352	63.19
	99.8	3.745(1)	5.119(3)	1.367	62.17
Te	0	4.451(1)	5.926(2)	1.331	101.67
	3.8	4.411(1)	5.934(2)	1.345	99.99
	6.0	4.398(1)	5.941(2)	1.351	99.52
	12.6	4.331(1)	5.951(2)	1.374	96.67
	14.8	4.312(1)	5.957(2)	1.381	95.92
	18.8	4.280(1)	5.967(2)	1.394	94.66
	22.6	4.258(1)	5.966(2)	1.401	93.68
	26.2	4.238(1)	5.969(2)	1.408	92.84
	29.4	4.225(1)	5.975(2)	1.414	92.37
	34.1	4.204(1)	5.972(2)	1.421	91.41
	38.2	4.191(1)	5.981(2)	1.427	90.98

TABLE II. Polynomal parameters A_{xn}, compression moduli B_x, and pressure derivatives B_x' for trigonal Se and Te.

	x	$10^5 A_{x1}$ (kbar^{-1})	$10^6 A_{x2}$ (kbar^{-2})	$10^8 A_{x3}$ (kbar^{-3})	B_x (kbar) This work	B_x (kbar) x-ray (Ref. 34)	B_x (kbar) x-ray (Ref. 8)	B_x (kbar) Neutron (Ref. 8)	B_x (kbar) Volume (Ref. 32)	B_x (kbar) Volume (Ref. 33)	B_x' This work	B_x' x-ray (Ref. 8)	B_x' Neutron (Ref. 8)	B_x' Volume (Ref. 32)	B_x' Volume (Ref. 33)
Se	a	−376(15)	42(6)	−19(5)	266(11)	175	331	290			4.9(12)	3.5	5.0		
	c	80(7)	−7(2)	3(1)	−1255(110)	−500	−629	−829			24(10)	20	38		
	V	−672(37)	77(7)	35(10)	149(9)	106	223	176	156	91	2.3(6)	1.2	1.9	4.3	2.3
					This work	x-ray (Ref. 29)		Ultr. (Ref. 10)	Lengths (Ref. 30)		This work				
Te	a	−273(5)	38(4)	−20(6)	366(8)	365		366	366		9(1)				
	c	39(5)	−5(3)	3(7)	−2590(300)	−2416		−2000	−2017		72(33)				
	V	−515(28)	8(2)	55(28)	194(10)	196		200	201		5.1(2)				

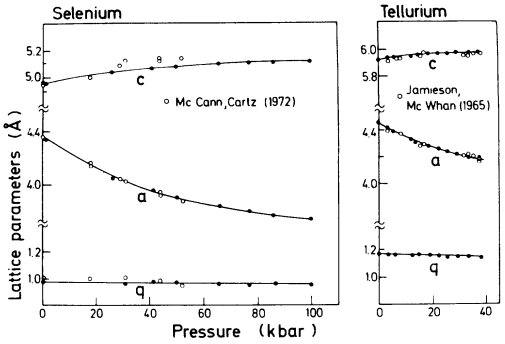

FIG. 3. Variation of the lattice parameters a and c and the atom-position parameter q for Se and Te under pressure.

in the coefficients of the polynomial fit include the error of the lattice-constant and pressure determination. The variation of a and c under pressure is shown in Fig. 3 and compared with earlier data for Se[11] and for Te.[29] It should be noted that the present data for Te agree well with the earlier results,[29-31] whereas the data for Se show significant differences, which may be related in fact to different bulk properties of the actual Se samples[32] and to nonhydrostatic strain effects in the previous studies. The present bulk modulus B_v of Se is in good agreement with the results of a piston cylinder high-pressure study,[32] where the density of the crystal had been measured also at atmospheric pressure and good agreement had been found with the x-ray density of the trigonal modification. The nonhydrostatic powder x-ray[8,34] and neutron studies,[8] on the other hand, give higher B_v values than the present results. The difference could result from the effects of encapsulation of the Se in NaCl.[8,32] This assumption is supported by the fact that the neutron data with a Se-to-NaCl mixture of 9 : 1 are in better agreement with our results than the x-ray data with an 18 : 1 mixture, and both values fit into the range between the present value of $B_v = 149$ kbar for Se and the value of $B_v = 237$ kbar for NaCl. Some of the earlier Se samples[33,34] may have in fact included amorphous contributions,[32] which were responsible for the low values of the respective bulk moduli. The pressure dependences of the dielectric constants $\epsilon_\perp$ and $\epsilon_\parallel$ as well as of some interband transition energies were derived recently[35,36] for Se from band calculations using empirical pseudopotentials and the literature values[8,37] for the bulk modulus of Se. The comparison of these results with recent reflectivity data[38] showed large discrepancies, which are reduced when the present data are used. A comparison of the present compressibility value for Se with elastic constants indicates that the literature values[37]

for $C_{11}+C_{12}$ and C_{33} would have to be increased by 30 and 10% to be consistent with the present compressibility value. The use of partly amorphous Se crystals in the previous measurements[37,39] could possibly account for these differences. The present values for the pressure dependence of the bulk modulus B_v' should be compared with previous results only in those cases where the B_v values themselves are consistent.[8,32] Therefore, the good agreement with some of the B_v' values is purely accidental.[33]

IV. VARIATION OF THE ATOMIC-POSITION PARAMETER

The determination of the atomic-position parameter u from the relative intensities includes corrections in polarization and Lorentz factors (PL) and for absorption effects. The PL correction was carried out using standard formulas[40] for the precession method. The absorption correction was based on an empirical formula.[27,41] Thereby, only absorption due to the crystal itself was taken into account, since the absorbing parts of the diamond anvil cell have approximately spherical symmetry as long as shadowing due to the gasket can be neglected. The absorption correction factors of Se and Te varied from 1.0 to 1.61 and from 1.0 to 2.49, respectively. Shadowing from the gasket was minimized by careful flat and central mountings of the crystals with respect to the diamonds and the whole in the gasket. Outer-most reflections which could have been affected by shadowing were eliminated when the intensities of equivalent reflections showed significant differences.

All structure calculations were performed on a Honeywell-Bull 66/60 computer using the x-ray system.[28] Since refined B factors showed strong statistical variations for Te, estimated B factors were used in this case. These values decreased from 1.27 to 0.81 under pressure. This variation affected the u parameter by only 0.1%.

In the structure calculations for Se, the isotropic B factor was used as free parameter, since the scatter of the B values was much smaller than in evaluations of the Te data. The B factors showed a systematic decrease from 2.0 at atmospheric pressure to 0.66 at 86.4 kbar. This decrease reflects, at least roughly, the increase of the Debye temperature for Se under high pressure. A standard weighting procedure was used in the evaluation of the Se data. The weighting factor was calculated from the observed structure factors F_{obs} by

TABLE III. Comparison of measured (F_{obs}) and calculated (F_{calc}) x-ray diffraction intensities and corresponding atom parameter u for trigonal Te under pressure. The asterisk denotes the zero-pressure literature values.[42]

p (kbar) \ hk	$\bar{1}03$		$\bar{1}02$		$\bar{1}01$		100		104		103		102		202	
	F_{obs}	F_{calc}	F_{obs}	F_{calc}	F_{obs}	F_{calc}	F_{obs}	F_{calc}	F_{obs}	F_{calc}	F_{obs}	F_{calc}	F_{obs}	F_{calc}	F_{obs}	F_{calc}
0		27.5		108.1		27.5		37.3		78.7		27.5		24.6		71.8
3.8	26.1	27.1	106.3	108.8	24.9	27.1	36.9	36.5	84.2	80.0	27.7	27.1	24.3	24.3	73.2	73.1
6.0	25.5	26.2	108.8	109.5	23.8	26.4	33.0	35.2	84.9	81.0	33.0	26.2	25.5	23.6	79.4	74.8
12.6	25.2	25.7	107.5	110.2	23.7	25.8	34.1	34.1	84.9	82.3	27.9	25.7	24.3	23.2	80.0	76.2
14.8	26.9	24.6	111.2	110.8	20.7	25.0	29.6	32.7	80.9	83.1	27.6	24.6	23.9	22.5	80.0	77.8
18.8	27.2	24.4	111.0	111.1	21.8	24.7	29.1	32.2	79.0	83.8	24.8	24.4	24.3	22.3	81.3	78.4
22.6	27.4	24.1	115.7	111.3	22.8	24.4	31.7	31.7	81.0	84.1	27.5	24.1	25.7	23.0	81.6	78.8
26.2	23.3	24.0	116.2	111.5	21.6	24.3	26.8	31.5	80.1	84.2	22.5	24.0	25.8	22.0	75.0	79.1
29.4	25.9	24.2	111.0	111.4	21.2	24.4	30.7	31.8	79.4	84.6	23.5	24.2	23.9	22.1	77.5	78.8
34.1	25.1	23.5	116.1	111.8	21.9	23.8	29.1	30.7	84.6	85.1	29.0	23.5	24.2	21.5	80.8	80.0
38.2	30.5	24.5	110.7	111.5	23.4	24.6	28.3	32.0	87.8	85.0	27.6	24.5	25.3	22.3	79.0	78.7

p (kbar) \ hk	201		200		$\bar{2}02$		$\bar{2}01$		003		R factor	u
	F_{obs}	F_{calc}	F_{obs}	F_{calc}	F_{obs}	F_{calc}	F_{obs}	F_{calc}	F_{obs}	F_{calc}		
0		57.4		33.9		53.0		77.7		106.3	···	0.2633*
3.8	56.4	56.4	31.5	33.8	54.8	52.3	79.9	78.8	105.8	107.1	0.025	0.2652(11)
6.0	53.3	54.6	32.1	33.4	50.3	50.7	74.7	80.5	107.3	107.6	0.044	0.2676(21)
12.6	55.3	53.2	33.5	33.1	48.3	49.6	80.2	81.7	106.9	108.4	0.030	0.2693(12)
14.8	51.7	51.1	29.8	32.5	47.6	47.7	80.6	83.4	111.5	108.7	0.038	0.2719(15)
18.8	50.4	50.5	30.2	32.3	46.9	47.2	79.5	83.9	115.6	109.1	0.045	0.2727(20)
22.6	48.3	49.8	31.3	32.1	42.3	46.5	78.8	84.3	110.4	109.3	0.049	0.2735(20)
26.2	46.7	49.5	27.4	32.0	50.5	46.3	82.5	84.5	111.1	109.5	0.056	0.2738(21)
29.4	47.5	50.0	31.8	32.1	47.0	46.7	82.5	84.2	117.9	109.7	0.039	0.2734(19)
34.1	44.2	48.3	32.6	31.5	44.2	45.2	80.4	85.3	109.6	109.8	0.042	0.2753(18)
38.2	44.2	50.2	34.4	32.2	47.6	47.1	80.4	83.9	111.7	110.0	0.048	0.2729(20)

TABLE IV. Comparison of measured (F_{obs}) and calculated (F_{calc}) x-ray diffraction intensities for trigonal Se under pressure. The asterisk denotes the zero-pressure literature values (Ref. 43).

p (kbar) \ $hk\cdot$	110		111		112		113		114		220		221		003		R	u
	F_{obs}	F_{calc}	F_{obs}	F_{calc}	F_{obs}	F_{calc}	F_{obs}	F_{calc}	F_{obs}	F_{calc}	F_{obs}	F_{calc}	F_{obs}	F_{calc}	F_{obs}	F_{calc}	factor	
0		41.5		37.5		32.7		28.1		20.7		20.0		21.3		58.0	...	0.2254*
25.8	42.6	43.3	30.7	32.1	26.5	27.8	28.8	28.5	17.2	16.8	10.1	11.6	12.7	18.0	56.7	56.0	0.052	0.2373(24)
41.5	48.3	48.0	30.4	29.9	26.3	26.3	22.9	33.2	14.8	16.9	11.0	10.4	21.3	19.9	58.4	58.5	0.021	0.2481(10)
49.9	52.3	50.6	34.7	31.3	29.8	28.2	37.4	37.6	22.0	19.9	16.2	12.5	25.0	24.3	61.0	62.9	0.055	0.2490(38)
65.7	54.3	52.8	36.1	32.7	31.2	30.2	42.1	41.9	24.7	23.2	18.7	14.8	28.7	29.1	65.5	67.1	0.044	0.2493(32)
77.0	53.7	52.0	36.3	32.7	29.4	30.1	41.2	41.2	26.7	23.1	18.6	14.5	26.8	28.3	65.3	66.8	0.056	0.2486(38)
86.4	55.2	52.1	34.0	37.7	29.0	30.2	40.9	41.5	24.7	23.3	21.6	14.6	26.7	28.5	63.3	67.2	0.069	0.2487(46)

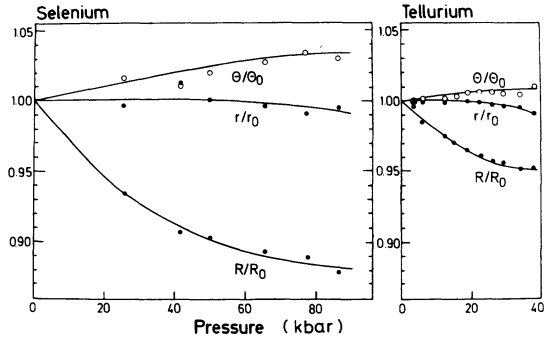

FIG. 4. Variation of the intrachain bond angle θ and of the intra- and interchain distances r and R for Se and Te under pressure.

$$W_{nkl} = F^2_{obs}(hkl)/F^2_{obs}(003)\,.$$

This weighting procedure allows for the fact that low-intensity reflections include larger relative errors in the evaluation of the films by the densitometer. The use of this procedure changed the u values typically by less than one standard deviation.

Tables III and IV represent the observed and calculated structure factors together with the reliability factor R and the resulting u parameter for Te and Se. Table III includes only the data for reduced data sets of 13 reflections, since the use of the complete data sets with different reflections being included for the different pressures increased only the scatter of the u value for Te.

The data of Se and Te in Tables III and IV show a strong increase of the atom-position parameter u under high pressure and a weakening of this increase from about 20 kbar for Te and from about 40 kbar for Se. The present standard deviations for the u values of <2% for Se and <1% for Te are considerably smaller than those given previously for Se.[11] The intra- and interchain distances r and R as well as the intrachain bond angle θ can be calculated from results given in the Tables I, III, and IV by the use of the relations

$$r = [3(ua)^2 + \tfrac{1}{9}c^2]^{1/2}\,,$$

$$R = [a^2(1-3u) + r^2]^{1/2}\,,$$

$$\theta = [2\cos^{-1}(3ua/2r)]\,.$$

The changes of these parameters under pressure are plotted for Se and Te in Fig. 4. The comparison with the earlier data[11] for Se indicates good agreement for the values of R and θ; however, the present data for r show no pronounced maximum at about 18 kbar.[11]

V. DISCUSSION

The major effect of pressure on the structure of Se and Te is definitely the strong decrease in the interchain distances which can be represented either as a strong decrease in the lattice constant a or in the interchain neighbor distance R. On the other hand, there is a very weak decrease in the chain radius $q = ua$ of about 0.1 Å in the pressure range from 0 to 90 kbar in Se and of about 0.04 Å from 0 to 40 kbar in Te. This decrease of q shows up in the initial pressure range as an increase of c and is responsible at higher pressure also for the increase of θ. The increase of the c/a ratio therefore represents primarily a decrease in the lattice anisotropy under pressure.

Previous investigations[9,10] on Se and Te indicated that the lattice dynamics of both elements follow closely a "homologous" behavior similar to the kind of homology that was noticed before for the group-IVB elements.[44,45] The homology implies in both cases that a simple scaling of masses, force constants, and lattice parameters sufficies to find "corresponding states" for the lattice dynamics of these elements. The difference in the c/a ratios for Se and Te at normal pressure and the homologous change in these c/a ratios with pressure were taken as support for the assumption that Se under pressure becomes more similar to Te.[10] Since the knowledge about the effect of pressure on the structural parameters of Se and Te was very limited,[11] some reasonable assumptions had to be made[9,10] to establish the close lattice-dynamical homology for Se and Te under pressure. The present data, however, allow for a detailed analysis of these assumptions.

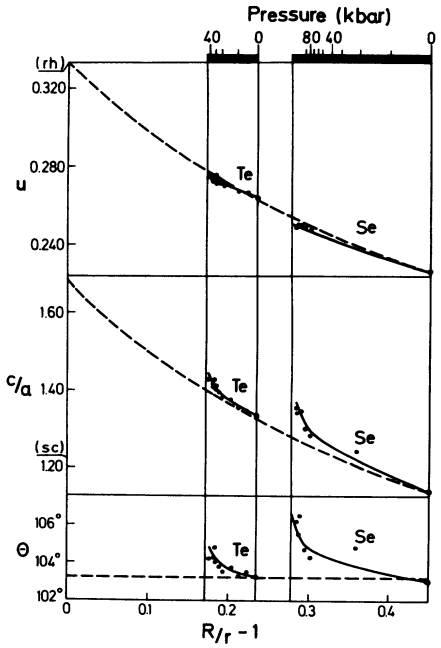

FIG. 5. Variation of the atomic-position parameter $u = q/a$, of the c/a ratio, and of the intrachain bond angle θ with respect to the anisotropy parameter $R/r - 1$ and comparison with the structural homology (dashed line).

Within these models,[3,4] a measure for the difference in the bonding within and between the chains is given by the anisotropy parameter $R/r - 1$. Equal inter- and intrachain bond lengths, i.e., $R/r - 1 = 0$, result in an atomic-position parameter $u = \frac{1}{3}$. This structure is rhombohedral with space group $R3m$-D_{3d}^5 and one atom at the origin of the rhombohedral unit cell.

The heavy lines in Fig. 5 show the actual variation of the atomic-position parameter u, of the c/a ratio, and of the intrachain bond angle θ for Se and Te with respect to the anisotropy parameter $R/r - 1$. The broken curves represent a homologous variation with constant $\theta = 103.2°$. Obviously, the deviations from this homologous variation are small at low pressure. Under higher pressures, for Se from about 40 kbar on and for Te from about 20 kbar on, deviations from the structural homology are seen most clearly in the variation of the bond angle with respect to $R/r - 1$.

For the following discussion of the approach to a structure with higher symmetry, only the hexagonal coordinate system is used. The variation of the atomic-position parameter u indicates that both Se and Te show only a slight tendency to approach the rhombohedral structure with $u = \frac{1}{3}$ and that the phase transitions into the metallic high-pressure phases at 140 kbar for Se,[46] and at 40 kbar for Te,[26] occur at values of u which are still far away from the rhombohedral value $\frac{1}{3}$. The variations of c/a and θ show no tendency to approach either the rhombohedral β-Po structure[45] ($u = \frac{1}{3}$, $c/a = 0.967$, $\theta = 81°$) or the simple-cubic α-Po structure ($u = \frac{1}{3}, c/a = \frac{3}{2} = 1.23, \theta = 90°$). The strong increases of both c/a and θ under pressure close to the phase transitions may therefore rather indicate a tendency to approach an fcc close packing of the atoms corresponding to $u \to \frac{1}{3}$, $c/a \to \sqrt{6} = 2.45$, and $\theta \to 120°$.

In fact, recent empirical-pseudopotential and tight-binding band-structure calculations[7] for Se and Te led also to the conclusion that the differences in the bonds within and between the chains should decrease strongly under pressure. Thereby, a strong increase in the admixture of d character to the bonding p orbitals should be responsible for the strong increase of the bond angle θ under pressure. From the fact that these changes result in strong deviations from the homologous variation of the lattice parameters for Se and Te

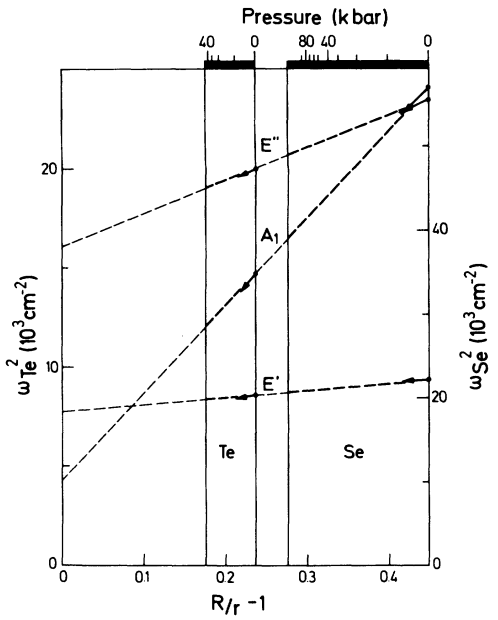

FIG. 6. Variation of the Raman frequencies (Ref. 9) with respect to the anisotropy parameter $R/r-1$ and comparison with the lattice-dynamical homology (dashed line).

under pressure, one may expect also strong deviations from the lattice-dynamical homology which was observed at low pressures.[10]

A perfect-lattice-dynamical homology for Se and Te would require[10,44,45] that all the phonon frequencies ω_n^{Se} of Se can be scaled to the values ω_n^{Te} of Te in "corresponding states" by only one empirical scaling factor,

$$S=(\omega_n^{Te}/\omega_n^{Se})^2(M^{Te}/M^{Se}),$$

independent of the mode and the k-vector index n, where M^{Te} and M^{Se} are the Te and Se masses, respectively. Within the valence-force-field (VFF) models,[4-6] the phonon frequencies ω_n are related to the force constants K_m by simple relations of the type

$$M\omega_n^2=\sum_m G_{nm}K_m,$$

where M stands for the mass of the atoms and the coefficients G_{nm} represent purely geometrical factors which depend for Se and Te, for instance, only on R/r and θ. If identical values of R/r and θ characterize the corresponding states of Se and Te, the homology of the frequencies therefore implies a similar homology of the force constants. To prove or disprove a lattice-dynamical homology of Se and Te, one has to compare the phonon frequencies of both substances in corresponding states. The discussion of the structural homology in the previous section showed in fact that hydrostatic pressures will not transform Se into a structural state which corresponds exactly to the structure of Te at low pressure. However, the deviations from the structural homology were small when the low-pressure data are extrapolated with respect to the anisotropy parameter $R/r-1$, under the assumption of no variation in θ. From this point of view, one expects that a lattice-dynamical homology may be observed only in simple extrapolations of the low-pressure data for the phonon frequencies. Furthermore, there is no physical reason to assume a linear variation of either the geometrical factors G_{nm} or the force constants K_m with respect to either pressure, volume, or anisotropy parameter $R/r-1$. If one assumes just for simplicity a linear variation of both the G_{nm}'s and the K_m's with respect to $R/r-1$, one obtains the linear variation of the squared phonon frequencies ω_n^2, which is used in Fig. 6 with the S value of the E' modes $S_E'=0.65$. Figure 6 points out clearly that in fact all pressure dependences of the Raman-active modes[9] in Se and Te follow closely this simple homology within the given accuracy and pressure range. The linear extrapolation of the A_1 mode far beyond the phase transitions in Se and Te indicates, however, that these phase transitions occur most likely before the A_1 and E' modes become degenerate, in contrast to an earlier extrapolation[3,9] which found a correlation between the transition pressures and the points where the A_1-E' splitting extrapolates towards zero. On the other hand, the present linear extrapolation leads still to an (unreasonable) crossover of the A_1 and E' modes at a finite value of $R/r-1$, whereas both modes should become degenerate only for vanishing anisotropy parameter. In fact, the strongly nonlinear variation of R/r with respect to pressure as well as the deviations of the bond angles θ from a constant value under high pressures (Fig. 5) pointed already to the fact that one should also expect nonlinear variations of the force constants and geometrical factors not only with respect to pressure, but also with respect to R/r as the phase transitions are approached.

This fact can be seen most clearly by inspection of the relation[3]

$$\frac{dr}{dp}\Big/\frac{dR}{dp}=\frac{2K_R-8QK_{rR}}{QK_r-8K_{rR}},$$

which correlates pressure derivatives of r and R with the geometrical factor $Q=(R/r)2u/(1-2u)$ and the three force constants K_r, K_R and K_{rR} of this VFF model.[3] From Fig. 4, one can infer that both the first and second derivatives of r with respect to pressure are very small at low pressures compared with the respective derivatives of R. This

experimental fact results in two conditions on the force constants at low pressures:

$$K_R \approx 4QK_{rR}, \quad K'_R \approx 4QK'_{rR} + 4Q'K_{rR},$$

whereby K'_R, K'_{rR}, and Q' represent the pressure derivatives at low pressures. The strong variation of r close to the phase transition can be accounted for within this model[3] by a finite value of the second derivative of at least one of the force constants. The large variation in R under pressure favors thereby a dominant contribution from K''_R. A finite (positive) value of this term would also account for a weaker decrease of the A_1 mode at higher pressures.

Raman measurements on Se and Te in an extended pressure range up to the phase transitions would definitely allow for a more quantitative test of the present VFF models, and should furthermore point out more clearly the limits of the lattice-dynamical homology.

ACKNOWLEDGMENTS

The authors are very grateful to G. J. Piermarini for his detailed advice on the diamond anvil technique and to G. Weiser and U. v. Alpen for supplying the single crystals of Se and Te, respectively. It is also a pleasure to acknowledge many stimulating discussions with M. Cardona, H. -J. Deiseroth, C. Irslinger, R. M. Martin, D. Schiferl, K. Syassen, and H. Wendel, as well as the excellent technical assistance of E. Böttcher, W. Dieterich, and W. König.

*Present address: ITT, 85 Nürnberg, Federal Republic of Germany.

[1]J. Donohue, *The Structure of the Elements* (Wiley, New York, 1974).

[2]P. Grosse, Springer Tracts Mod. Phys. 48 (1969).

[3]R. M. Martin and G. Lucovsky, in *Proceedings of the Twelfth International Conference on the Physics of Semiconductors, Stuttgart, 1974* (Teubner, Stuttgart, 1974), p. 184.

[4]R. M. Martin, G. Lucovsky, and K. Helliwell, Phys. Rev. B 13, 1383 (1976).

[5]H. Wendel, W. Weber, and U. D. Teuchert, J. Phys. C 8, 3737 (1975).

[6]T. Nakayama and A. Odajima, J. Phys. Soc. Jpn. 34, 732 (1973).

[7]J. D. Joannopoulos, M. Schlüter, and M. L. Cohen, Phys. Rev. B 11, 2186 (1975).

[8]D. R. McCann, L. Cartz, R. E. Schmunk, and Y. D. Harker, J. Appl. Phys. 43, 1432 (1972).

[9]W. Richter, J. B. Renucci, and M. Cardona, Phys. Status Solidi B 56, 223 (1973).

[10]T. A. Fjeldly and W. Richter, Phys. Status Solidi B 72, 555 (1975).

[11]D. R. McCann and L. Cartz, J. Appl. Phys. 43, 11 (1972); 43, 4473 (1972).

[12]U. V. Alpen (private communication).

[13]J. D. Persio, J. C. Doukhan, and G. Saada, Mater. Sci. Eng. 4, 123 (1969).

[14]H. E. Swanson and E. Tatge, Natl. Bur. Stand. (U.S.) Report, 1951 (unpublished)

[15]G. Weiser (private communication).

[16]H. E. Swanson, N. T. Gilfrich, and G. M. Ugrinic, Natl. Bur. Stand. (U.S.) Circ. 5, 539 (1955).

[17]C. E. Weir, E. R. Lippincott, A. V. Valkenburg, and E. N. Bunting, J. Natl. Bur. Stand. (U.S.) 63A, 55 (1959).

[18]G. J. Piermarini and C. E. Weir, J. Natl. Bur. Stand. (U.S.) 66A, 4 (1962).

[19]C. E. Weir, G. J. Piermarini, and S. Block, Rev. Sci. Instr. 40, 1133 (1969).

[20]R. A. Forman, G. J. Piermarini, J. D. Barnett, and S. Block, Science 176, 284 (1972).

[21]R. Keller and W. B. Holzapfel, Rev. Sci. Instr. 48, 517 (1977).

[22]J. D. Barnett, S. Block, and G. J. Piermarini, Rev. Sci. Instr. 44, 1 (1973).

[23]G. J. Piermarini, S. Block, and J. D. Barnett, J. Appl. Phys. 44, 5377 (1973).

[24]G. J. Piermarini, S. Block, J. D. Barnett, and R. A. Forman, J. Appl. Phys. 46, 2774 (1975).

[25]D. Schiferl (private communication).

[26]G. C. Kennedy and P. H. LaMori, J. Geophys. Res. 67, 851 (1962).

[27]R. Keller, thesis (Stuttgart, 1975) (unpublished).

[28]J. M. Steward, G. J. Kruger, H. L. Ammon, C. Dickinson, and S. R. Holl, University of Maryland Technical Report No. TR-192, 1972 (unpublished).

[29]P. W. Bridgman, Proc. Am. Acad. Arts Sci. 60, 303 (1925).

[30]J. C. Jamieson and D. B. McWhan, J. Chem. Phys. 43, 1149 (1965).

[31]J.-L. Malgrange, G. Quentin, and J.-M. Thuillier, Phys. Status Solidi 4, 139 (1964).

[32]A. K. Singh and G. C. Kennedy, J. Phys. Chem. Solids 35, 1545 (1974).

[33]P. W. Bridgman, Proc. Am. Acad. Arts Sci. 74, 21 (1940).

[34]L. F. Vereshagin, S. S. Kabalkina, and B. M. Shulenin Dokl. Akad. Nauk SSSR 165, 297 (1965) [Sov. Phys. Dokl. 10, 1053 (1966)].

[35]M. Wendel, R. M. Martin, and D. J. Chadi, Phys. Rev. Lett. 38, 656 (1977).

[36]J. D. Joannopoulos, Th. Starkloff, and M. Kastner, Phys. Rev. Lett. 38, 660 (1977).

[37]R. M. Martin, T. A. Fjeldly, and W. Richter, Solid State Commun. 18, 865 (1976).

[38]M. Kastner and R. R. Forberg, Phys. Rev. Lett. 36, 740 (1976).

[39]J. Mort, J. Appl. Phys. 38, 3414 (1967).

[40]J. Waser, Rev. Sci. Instr. 22, 8 (1951).

[41]B. Morosin and J. E. Schirber, Phys. Lett. A 30, 512 (1964).

[42]P. Cherin and P. Unger, Acta Cryst. 21, A46 (1966).

[43]P. Cherin and P. Unger, Acta Cryst. 23, 670 (1967).

[44]R. I. Kuchev, Fiz. Tverd. Tela 4, 2385 (1962) [Sov. Phys. Solid State 4, 1747 (1963)].

[45]G. Nilson and G. Nelen, Phys. Rev. B 6, 3777 (1972).

[46]D. R. McCann and L. Cartz, J. Chem. Phys. 56, 2552 (1972).